

Numerical analysis of FRAP experiments for DNA replication and repair

Eugenio Cinquemani, Vassilis Roukos, Zoi Lygerou and John Lygeros

Abstract—In this paper we describe a stochastic model for particle diffusion and binding within cell nuclei, and a numerical approximation of it that is well suited for numerical simulation and investigation of Fluorescence Recovery After Photobleaching (FRAP) experiments. An overview of the theory and of the implementation of the method is given. Simulation results are reported and are used to analyze data from real photobleaching experiments, mainly at a qualitative level.

Index Terms—Biological systems, Monte Carlo methods, Numerical simulation, Stochastic approximation, Parameter identification

I. INTRODUCTION

The genetic content of all eukaryotic cells must remain unaltered during the cell's life cycle and be accurately passed down to the daughter cells. Nuclear proteins constantly scan the genome to ensure that any damage on the DNA is quickly identified and repaired. Similar protein assemblies ensure that the complete genome is replicated once and only once per cell cycle. Assessing the dynamic interactions which lie at the heart of the maintenance of genomic stability is pivotal for an understanding of the normal mechanisms which keep the genome intact and how aberrations in these mechanisms may lead tumorigenesis. The highly dynamic nature of these interactions calls for methods which permit an assessment of protein-protein and protein-DNA interactions and modifications within the context of the living cells, and for analytical tools which will enable the nature of these interactions to be fully grasped.

Functional live cell imaging techniques, such as Fluorescence Recovery After Photobleaching (FRAP), Photoactivation and Fluorescence Correlation Spectroscopy (FCS), track fluorescently labeled proteins of interest within living cells [20], [9], [8]. Data analysis permits the dynamic behavior of these proteins to be assessed [16], [18], [25]. Modelling of the underlying molecule movements and interactions permits quantitative information to be extracted from the data collected, leading to an assessment of protein diffusion rates, interactions, on-off rates and subunit composition under different experimental conditions. These quantitative data can then be used for modelling of the biological processes under study. These techniques are increasingly used by cell biology

This research has been supported by the European Commission under project HYGEIA (NEST-4995).

E. Cinquemani and J. Lygeros are with the Automatic Control Laboratory, ETH Zurich, Switzerland.

V. Roukos and Z. Lygerou are with the School of Medicine, University of Patras, Greece.

Corresponding author: Eugenio Cinquemani, ETL K12, Physikstrasse 3, 8092 Zurich, Switzerland (cinquemani@control.ee.ethz.ch).

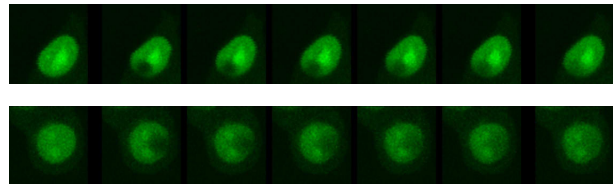


Fig. 1. FRAP experiments in living cells. Above: Cdt1 tagged with Green Fluorescent Protein (Cdt1GFP) from jellyfish *Aequorea victoria*. Below: GFP-tagged Cdt1 mutant (Cdt1 Δ 1-140GFP) with reduced binding affinity.

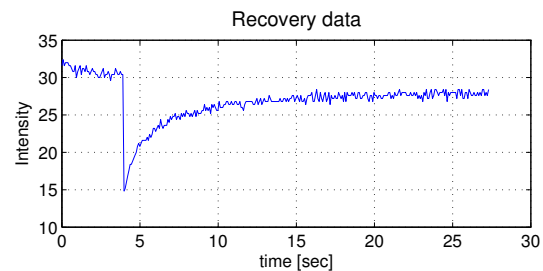


Fig. 2. Non-normalized FRAP curve from experimental data.

laboratories, and developing robust methods for data analysis and parameter identification will be of interest to a wide community.

During Fluorescence Recovery After Photobleaching analysis, naturally fluorescent proteins (tags) are attached to one or more proteins of interest and possibly some carefully chosen mutants, and laser microscopy is used to bleach (high-intensity pulse) part of the tags and observe (low-intensity scanning) fluorescence recovery in the region of interest after the bleaching (see images in Figure 1 and the computed recovery curve in Figure 2 – data are courtesy of G. Xouri, EMBL Heidelberg).

Conventional analysis techniques, pioneered in [1], rely heavily on model simplification to derive tractable mathematical expressions or reference recovery curves that can be fitted to the data analytically or at a low computational cost. Several such models have been proposed in recent years [17], [15], [16], [7], [3], [6] which make specific assumptions to simplify analysis. However, this simplicity comes at the cost of limited or no spatial resolution in the description of the diffusion-binding processes and of an incomplete exploitation of the data. In addition, it has been realized that concentration-type approaches reach their limits when the size of the particle population being considered is not sufficient, which is often the case in the context of our interest. On the other hand, computational technologies

are becoming mature for the simulation of highly realistic models of diffusion and binding reactions of macromolecules within the cell nucleus [2], [21]. These can be used to perform *in silico* FRAP experiments, whence to carry out analysis and identification of protein diffusion and binding mechanisms by way of qualitative or quantitative data matching.

Molecule dynamics within cells show clear hybrid characteristics with continuous molecule movement due to diffusion, and changes in molecule states due to interactions. Our aim is to model diffusion and binding at a particle level, by taking into account explicitly the stochastic nature of diffusion and binding interaction events. A similar approach is taken in [23], [24] for the simulation of biochemical networks. Based on the model, we wish to provide numerical tools for the random execution and, possibly, for the theoretical investigation of the model. Ultimate aim of our work is to exploit model analysis and simulation to perform identification of unknown parameters, such as binding propensities and diffusion coefficients, and verification (model validation) of biological hypotheses.

In Section II we define the stochastic model of diffusion and binding of proteins within the cell's nucleus. In Section III we describe the discrete approximation of this model on a time-space grid. Numerical simulation of FRAP experiments by way of this model approximation is discussed in Section IV. In Section V, simulation results are compared with real data from FRAP experiments on living cells expressing the replication protein Cdt1. Cdt1 is a crucial member of a multiprotein complex that regulates when and where DNA replication takes place, ensuring that DNA replication initiates from specific sites on chromatin only once per cell cycle [4], [5], [13], [25]. Final comments and perspectives of our work are reported in Section VI.

II. MODELLING OF PROTEIN DIFFUSION AND BINDING

As a first step toward the analysis of DNA maintenance processes, we wish to model protein diffusion within the nucleus and binding to sites along the DNA. This is done at a particle level. We begin by considering the following setting:

- N copies of one protein are present within the nucleus of one cell;
- the nucleus has a 3-dimensional ellipsoidal shape;
- protein molecules do not cross the boundaries of the nucleus;
- when a molecule is not bound, it can move in a way that is isotropic and independent from the location within the nucleus; moreover, it has a probability of binding to a DNA site that is uniform over the nucleus;
- when a molecule is bound, it does not move and it has a probability of unbinding that is uniform over the nucleus;
- molecules diffuse and bind independently of each other.

In particular, the assumption that the nuclear boundary is impermeable is valid in the cell's initial growth phase for

the protein that will be considered in Section V [14]. On the other hand, it was observed that protein-protein interactions that increase the mass of a protein cannot change its diffusion significantly [22], [15]. These qualitative assumptions are translated in the following mathematical model. Let $t \in \mathbb{R}$ denote time and $p = [x \ y \ z]^T \in \mathbb{R}^3$ denote spatial coordinates in a three-dimensional space. Let $p_i(t) = [x_i(t) \ y_i(t) \ z_i(t)]^T$, with $i = 1, \dots, N$, denote the position of the i -th molecule at time t . It is assumed that, at all t and for all i , $p_i(t) \in \mathcal{N}$, where $\mathcal{N} = \{p \in \mathbb{R}^3 : (p-c)^T S (p-c) \leq 1\}$ is an ellipsoidal domain that describes the cell nucleus ($c \in \mathbb{R}^3$ is the center of the ellipsoid and $S \in \mathbb{R}^{3 \times 3}$ is a positive definite matrix that describes the shape of the ellipsoid). For $i = 1, \dots, N$, let $q_i(t) \in \{0, 1\}$ be the mobility state of the molecule i at time t : $q_i(t) = 0$ if the molecule is unbound, $q_i(t) = 1$ if the molecule is bound. Whenever $q_i(t) = 1$ molecule i cannot move, whence we describe its dynamics by the following differential equation:

$$\dot{p}_i(t) = 0.$$

Conversely, when $q_i(t) = 0$, molecule i is allowed to move. In this case, as long as the molecule i is not hitting the boundary of \mathcal{N} , we assume that its position obeys the driftless diffusion

$$dp_i(t) = DdB_i(t), \quad (1)$$

where D is a diffusion matrix coefficient and stochastic process $B_i(t)$ is a standard (three dimensional) Wiener process (Brownian motion), having mean zero and covariance equal to the identity matrix I . Since the diffusion is assumed to be isotropic, we assume that $D = \sigma I$, for some $\sigma > 0$. The effect of the boundary $\partial\mathcal{N} = \{p \in \mathbb{R}^3 : (p-c)^T S (p-c) = 1\}$ on the dynamics of molecule i are formally accounted for by an additional "reflection" process R_i that "counteracts" any attempt of process $p_i(t)$ to leave domain \mathcal{N} . Therefore, equation (1) is rewritten as follows [10]:

$$dp_i(t) = DdB_i(t) + dR_i(p_i(t)),$$

where, loosely speaking, $dR_i = 0$ if $p_i(t) \in \mathcal{N} \setminus \partial\mathcal{N}$, and is a suitable nonzero vector along the inward normal to $\partial\mathcal{N}$ at $p_i(t)$ if $p_i(t) \in \partial\mathcal{N}$. The effect of process R_i is to convert variations of p_i towards the outside of \mathcal{N} into a sliding of p_i along $\partial\mathcal{N}$. In a more compact form, the dynamics of molecule i are expressed by the following switching diffusion:

$$dp_i(t) = \sigma_{q_i(t)} IdB_i(t) + dR_i(p_i(t)),$$

where $\sigma_q = \sigma$ if $q = 0$, and $\sigma_q = 0$ otherwise. Finally, the evolution of process $q_i(t)$, describing the binding events of molecule i , follows the laws of a continuous-time binary Markov chain. In particular, the probabilities that molecule i binds to/unbinds from a DNA site in the infinitesimal time interval $[t, t + \delta t)$ is expressed by the relations:

$$\begin{aligned} \mathbb{P}[q(t + \delta t) = 1 | q(t) = 0] &= \lambda_{bind} \delta t + o(\delta t), \\ \mathbb{P}[q(t + \delta t) = 0 | q(t) = 1] &= \lambda_{release} \delta t + o(\delta t), \end{aligned} \quad (2)$$

where $\lambda_{bind} \geq 0$ and $\lambda_{release} \geq 0$ quantify the bind and release propensities, respectively, and $o(\delta t)$ are higher order terms. Let T_{imm} be the expected immobilization time of a particle, and F_{imm} be the expected fraction of immobile population. It can be shown that, under stationary conditions,

$$T_{imm} = 1/\lambda_{release},$$

$$F_{imm} = \lambda_{bind}/(\lambda_{bind} + \lambda_{release}).$$

Similar formulas are found in the literature for different models of particle diffusion and binding (see e.g. [6], [25]). Several extensions of this model are rather straightforward. In particular, we have already considered the following:

- Diffusion coefficients and probabilities of binding/unbinding that depend on the position within the nucleus (e.g. being different within a nucleolus). This amounts to consider space-dependent diffusion coefficients $\sigma_q(p)$ and transition rates $\lambda_{bind}(p)$ and $\lambda_{release}(p)$, with $p \in \mathcal{N}$;
- Several different proteins that do not interact. This can be implemented by defining different diffusion coefficients, transition rates and number of molecules for different protein species.

Other extensions can be promptly implemented. On the other hand, interaction between proteins of the same or different species, and specific recruitment mechanisms onto DNA, are nontrivial from the modelling viewpoint, and need further investigation. A convenient approximation of the above model that is well suited to include such extensions is described below.

III. APPROXIMATION ON A GRID

Numerical approximation is needed in order to simulate and study the model presented above. Out of several reasonable approximations, we chose to follow the approximation method introduced in [10] for jump diffusion processes and revisited in [19] in the context of stochastic hybrid systems. The method is based on the idea of gridding both the state-space and time according to a gridding parameter $h > 0$, the meaning of which will be clarified below, and to build a discrete-state discrete-time Markov chain that converges in distribution to the original continuous-time, continuous-state stochastic process as $h \rightarrow 0$. Contrary to the implementations in [10], [19], that would require to grid the whole $3 \times N$ -dimensional continuous state-space of the model, here we grid the “physical” 3-dimensional space and approximate the diffusion of particles on the same space grid. This choice does not impair the approximation accuracy and yields a great complexity reduction. In perspective, it will facilitate the implementation of particle interactions (e.g. two particles will be candidates for interaction if they happen to meet at the same point of the grid, or within a convenient set of neighboring points) and possibly the analytic investigation of the discretized model.

Without going into too much technical detail (interested readers are deferred to [19]), one starts by defining the space grid as $h \times \mathbb{Z}^3$ (where \mathbb{Z} is the set of integers) and discrete

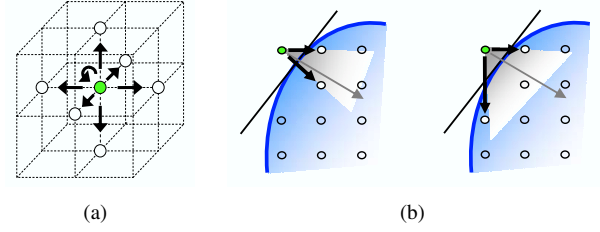


Fig. 3. (a) Approximation of particle diffusion on a three-dimensional space grid. Arrows represent the possible moves of a particle i from point p_i to neighboring points $p_i + z$ at distance h . (b) Alternative choices (left and right drawings) for the approximate reflection of a particle at the boundaries. The blue shaded region and the blue thick curve represent the domain \mathcal{N} and its boundary $\partial\mathcal{N}$. The thick black arrows represent possible moves $\mathcal{R}(p_i)$ inside \mathcal{N} of particle i that lies at a point p_i outside \mathcal{N} . The thin gray arrow represents the desired direction of reflection v , which is normal to the tangent (thin black line) of $\partial\mathcal{N}$ at a point close to p_i . Moves $\mathcal{R}(p_i)$ must be chosen so that the enclosed (gray shaded) region contains v .

time instants t_k such that the $t_{k+1} - t_k$ are independent exponentially distributed random variables with mean $T = \rho h^2$. Constant ρ must satisfy $0 < \rho \leq \bar{\rho}$, where the upper bound $\bar{\rho}$ depends on the maximum value taken on by σ over the space of interest. The choice of sampling the dynamics at random times facilitates the proof of convergence of the numerical approximation, however it is not essential [10]. To fix the ideas, we shall assume from now on that $t_k = kT$. Next one defines the probability that a molecule i sitting at a point $p_i \in h\mathbb{Z}^3$ at time kT , with $k \in \mathbb{Z}$, will jump to a neighboring point $p_i + z$ at time $(k+1)T$, for all $z \in \{[0 \ 0 \ 0], [\pm h \ 0 \ 0]^T, [0 \ \pm h \ 0]^T, [0 \ 0 \ \pm h]^T\}$ (see Fig. 3(a)). These probabilities depend on σ , on the mobility status $q_i(kT)$ and on the constant ρ . For σ independent of p_i and $q_i(kT) = 0$, the case $\rho = \bar{\rho}$ corresponds to the case where $\mathbb{P}[z = [0 \ 0 \ 0]^T] = 0$, i.e. particles must move at all discrete time instants. Then, one defines the probabilities of transition $\mathbb{P}[q_i((k+1)T) = 1 | q_i(kT) = 0]$ and $\mathbb{P}[q_i((k+1)T) = 0 | q_i(kT) = 1]$ as a function of the propensities λ_{bind} and $\lambda_{release}$ and of T (by way of equation (2), with T in place of δt and $o(\delta t) \simeq 0$). Contrary to what suggested in [10], in our setting a particle of the discretized model is allowed to both move and bind in the transition from time kT to time $(k+1)T$. This ensures that the approximation is better behaved for non-infinitesimal values of h . A formal proof of the asymptotic convergence of this modified discrete approximation to the original continuous model is being developed. Finally, the reflection process that guarantees that particles are confined within boundaries is approximated as follows. If, in a move from time kT to time $(k+1)T$, a particle falls into a grid point p_i outside of the boundaries, it is instantaneously reflected back into the $\{h\mathbb{Z}^3\} \cap \mathcal{N}$ domain along the normal v to $\partial\mathcal{N}$ at a point $p^* \in \partial\mathcal{N}$ “close enough to” p_i . In general, though, the intersection $\{p_i + \alpha v : \alpha \in \mathbb{R}\} \cap (h \times \mathbb{Z}^3 \cap \mathcal{N})$ is empty (no grid point internal to \mathcal{N} is found along direction v from p_i). The way to circumvent this is to define a set of candidate reflection points $\mathcal{R}(p_i) \subset h\mathbb{Z}^3 \cap \mathcal{N}$ and reflection probabilities $\mathbb{P}[p]$,

with $p \in \mathcal{R}(p_i)$, so that

$$\mathbb{E}[p_i((k+1)T)] = \sum_{p \in \mathcal{R}(p_i)} p \cdot \mathbb{P}[p] \in \{p_i + \alpha v : \alpha \in \mathbb{R}\}$$

(see Fig. 3(b)). This states that, on average, the particle violating the constraint is reflected back into \mathcal{N} along the normal to $\partial\mathcal{N}$ at p^* . In practice, this is implemented by extracting the reflection point at random according to the probability distribution $\mathbb{P}[p]$, $p \in \mathcal{R}(p_i)$. For asymptotic consistency, it is sufficient to ensure that, when $h \rightarrow 0$, $p^* \rightarrow p_i$ and all points $p \in \mathcal{R}(p_i)$ approach the boundary $\partial\mathcal{N}$.

IV. MODELLING OF FRAP EXPERIMENTS

GFP fusion proteins are ideal for use in FRAP studies because they can be photobleached without damaging the molecule or the cell [12], suggesting that also the dynamics of diffusion and the binding properties of the bleached molecules are not affected. Therefore, in our model we make the standard assumption that either tagging and bleaching do not affect the dynamics of diffusion and binding of the molecules of interest [11]. To account for the labelling of protein molecules with fluorescent tags, for each molecule i , we consider a binary variable $f_i(t)$, which takes value 1 if the tag at time t is fluorescent, and 0 if it is not. One may assume that, at the beginning of an experiment, all tags are fluorescent, i.e. $f_i = 1$ for all i . Photobleaching experiments are modelled as follows. A three-dimensional region \mathcal{B} within nucleus \mathcal{N} is defined to describe the volume that is bleached by the high intensity laser pulse. This volume is currently described as a sphere, but it could easily be generalized to more accurate (e.g. conical [20]) descriptions of the bleaching profile. A time interval $[t_b, t_b + \tau_b)$ is defined to represent the activation of the bleaching pulse. In the time course of a simulation experiment, random execution of the discrete-time discrete-space model simulates the diffusion of the particles within the cell nucleus. All particles that enter the bleaching region when bleaching is active get bleached with a probability that is proportional to the time spent in the bleaching region. This is captured in the model by assuming that the evolution of f_i is governed by a Markov chain with transition probability laws that depend on t and on p_i and are independent of q_i . More specifically, let $r_{bleach}(p_i, t)$ be the rate of transition from 1 to 0. We define

$$r_{bleach}(p_i, t) = \begin{cases} 0, & \text{if } t \notin [t_b, t_b + \tau_b) \text{ or } p_i \notin \mathcal{B}, \\ b_{eff}, & \text{if } t \in [t_b, t_b + \tau_b) \text{ and } p_i \in \mathcal{B}, \end{cases}$$

where $b_{eff} > 0$ is the bleaching efficiency. On the other hand, we currently assume that, once bleached, a tag does not recover fluorescence. This is modelled by setting the rate of transition from 0 to 1 equal to zero. In future developments, phenomena such as temporary tag bleaching could be taken into account by a suitable modification of these laws. In practice, this model is cast in the discrete-time simulation scheme of Section III by ensuring that, if $p_i(t) \in \mathcal{B}$ at a time $t_k \in [t_b, t_b + \tau_b)$ then $f_i(t)$ is set to 0 with probability $T \times b_{eff}$.

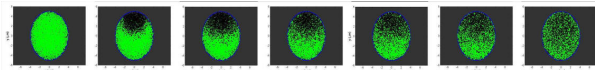


Fig. 4. Simulation of diffusion and binding of 10000 particles within a 3D ellipsoidal domain (2D view). Simulation of a 27.3-seconds experiment (350 FRAP images) currently takes 1–5 hours depending on the system parameters. Time step is 0.008 seconds, space resolution is $0.1\mu\text{m}$.

Observation of the evolution of fluorescence during the time course of the experiment is defined as follows. A sequence of imaging time instants $T_{sample} \times \mathbb{Z}$ is defined, where $T_{sample} > 0$ is the time between observations (note that in general $T_{sample} \neq T$). At every time $t \in T_{sample} \times \mathbb{Z}$, the number of fluorescent particles (i.e. such that $f_i(t) = 1$) within one or multiple three dimensional regions (e.g. a spherical region of interest and the whole \mathcal{N}) are counted separately. This count is taken as a measure of the fluorescence intensity. In practice, given that the simulation times are discrete, the fluorescence state of molecules at the simulation time t_k closest to t is considered. In order to guarantee an accurate approximation, of course, it must hold that $T \ll T_{sample}$. In fact, the current implementation of the simulator records the complete status of the simulation at all observation times, so that information such as fluorescence intensity profiles in arbitrary regions of the nucleus can be inferred by data post-processing. On the other hand, at present, bleaching of the region of interest is part of the simulation, and cannot be modified by postprocessing.

V. SIMULATION RESULTS

In this section we shall describe the results obtained by simulating FRAP experiments with a realistic experimental setting derived from [25]. In the following, unless specified otherwise, lengths are measured in microns (μm) and time in seconds (s). We considered the dynamics of nuclear-localized protein Cdt1 in a nucleus modelled as an ellipsoid with x , y , and z axis diameters equal to 10, 8 and $8\mu\text{m}$, respectively. Observations of fluorescence are taken every $T_{sample} = 0.078\text{s}$, for a total of 351 measurements over the time span $[0, 27.3]\text{s}$. Unless otherwise stated, the Region Of Interest (ROI), where fluorescence recovery is observed, and the bleaching region coincide and are modelled as a sphere with diameter $4\mu\text{m}$. As explained above, fluorescence at time t is measured by counting the number of particles such that $f_i(t) = 1$. This is done for both the ROI and the total nuclear volume scanned by the low-intensity laser. The latter is, in first approximation, the whole cell nucleus. A pictorial example of the simulation of a FRAP experiment is given in Fig.4, where one pre-bleaching and several post-bleaching 2-dimensional views of fluorescent (green spots) vs. bleached (black spots) particles are reported. Population size is fixed to $N = 10000$. As will be evident below, this leads to a noise level for the fluorescence recovery curves that is comparable to what observed experimentally on a single cell. The gridding parameter is fixed to $h = 0.1\mu\text{m}$ in all experiments, leading to a dynamics sampling time T in the order of 10^{-3}s . At this stage, due to the computational

burden of the method (at the given level of accuracy, one simulation takes between 1 and 5 hours, depending on the diffusion coefficients – the faster the diffusion, the longer the simulation time), the conclusions we are able to draw are mainly qualitative. Yet the flexibility and the spatial resolution of the method already enable us to investigate certain aspects of FRAP experiments that cannot be studied by conventional analytic or numerical methods.

A. FRAP experiments on *Cdt1*

In this experiment we replicate part of the simulation experiments described in [25] (see Figure 2 thereof and the section Materials and Methods, subsections FRAP experiments and FRAP data analysis). We first simulated diffusion and binding with coefficients λ_{bind} and $\lambda_{release}$ such that $F_{imm} = 20\%$ and $T_{imm} = 64s$, and a diffusion coefficient $\sigma = 1.9\mu m/s$. Next we repeated the simulation with parameters such that $F_{imm} = 0\%$ (in this case T_{imm} is irrelevant) and with $\sigma = 4.8\mu m/s$. According to [25], these two parameterizations are those that best explain the observed data for *Cdt1* and its non-binding mutant *Cdt1* $\Delta 1 - 140$. Results are reported in Figure 5. *Cdt1* recovery is plotted in blue (simulated) and black (experimental data), whereas *Cdt1* $\Delta 1 - 140$ recovery is plotted in red (simulated) and green (experimental data). Experimental data were provided to us by G. Xouri, EMBL Heidelberg. In both cases, we plotted the Normalized Recovery Curves (NRI), which were computed as explained in [25]. It can be seen that, according to our simulator, the velocity of recovery of *Cdt1* $\Delta 1 - 140$ is overestimated in [25], whereas the mobility of *Cdt1* is underestimated. In addition, the simulated NRI curve for *Cdt1* does not recover the value 1 by the end of the experiment. This means that the fluorescence in the ROI is still lower than the average fluorescence of the cell nucleus. Indeed, this should be expected since, for $T_{imm} = 64s$, a large portion of the bleached molecules is likely to be still immobilized within the bleaching region at the final time of the experiment (27.3s), and suggests that a $T_{imm} = 64s$ may be too large for *Cdt1*. On the other hand, for *Cdt1* $\Delta 1 - 140$, the effective diffusion may be slower than estimated, which would suggest lower values of σ or more binding affinity (larger λ_{bind} or smaller $\lambda_{release}$). We note however that normalized experimental data have been used for our comparisons, and over-normalization could partly account for the loss of an obvious immobile fraction. In addition the effect of the shape of the bleached region used for simulations (here simplified as a sphere) should be investigated. Further analysis using our model will hopefully allow for an accurate estimation of binding and diffusion parameters for *Cdt1*.

B. Diffusion and binding in nucleoli

In this experiment we studied the recovery of fluorescence within nucleoli. We conducted experiments on mammalian cancerous cells (breast cancer MCF7 cells). Cells seeded on MatTek dishes were grown in DMEM/high glucose with 10% (v/v) fetal bovine serum and were transfected with a plasmid expressing *Cdt1* tagged with GFP using Fugene 6 (Roche)

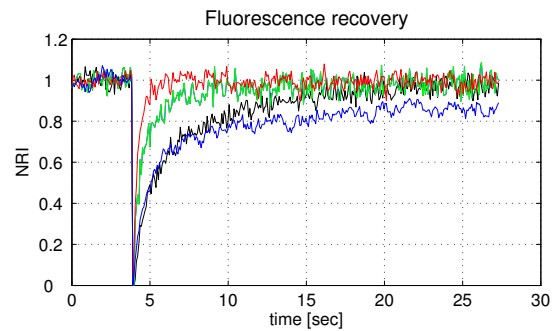
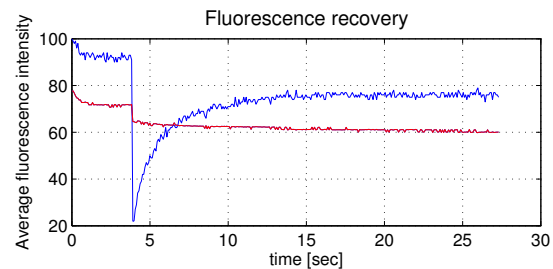
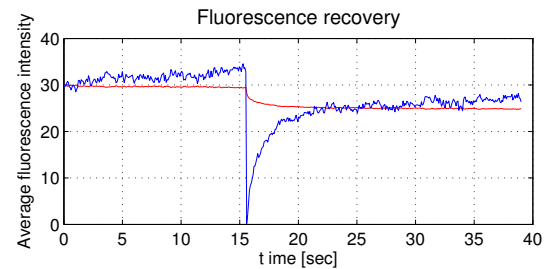


Fig. 5. FRAP curves of *Cdt1* (black=true, blue=simulated) and its mutant *Cdt1* $\Delta 1 - 140$ with reduced binding affinity (green=true, red=simulated).



(a) Experimental data.



(b) Simulation.

Fig. 6. FRAP curves inside (blue) and outside (red) a bleached nucleolus.

according to manufacturer instructions. 22 hours following transfection FRAP experiments were performed on a Leica SP5 confocal microscope equipped with an X 63/1.4NA oil immersion lens. First, the observation of steady state fluorescence levels revealed larger concentration of *Cdt1* (i.e. higher fluorescence intensity) within nucleoli than in the rest of the nucleus. This suggests higher binding affinity or an increased number of binding sites within nucleoli. Then fluorescence recovery after bleaching was recorded. Fifty pre-bleaching images were obtained every 0.066s followed by single bleach in a circular ROI covering most of a nucleolus (diameter $\approx 4\mu m$) and by 300 post-bleach images recorded at 0.066s intervals. The fluorescence recovery curve in a bleached nucleolus is reported (without normalization) in Figure 6(a) (blue) along with the variation of intensity outside of the nucleolus (red). To assess whether an increased binding affinity within nucleoli can explain the experimental curves of Figure 6(a) we simulated an experiment where a spherical nucleolus of diameter $4\mu m$ is bleached and variations of fluorescence intensity are observed inside and outside of the

nucleolus. Binding/unbinding propensities are assigned so that, outside of the nucleolus, $T_{imm} = 1$ and $F_{imm} = 0.1$, whereas the binding propensity λ_{bind} is doubled within the nucleolus. The resulting curves of fluorescence intensity are reported (without normalization) in Figure 6(b). Note that, in simulation, a longer pre-bleaching period is considered, to allow the distribution of fluorescent molecules to approach stationarity (in the initialization of the simulation, molecules are equally distributed throughout the nucleus; since λ_{bind} is location-dependent, this is not a stationary condition for the system). This is reflected in the variations of intensity prior to bleaching. Qualitative comparison of Figures 6(a) and 6(b) suggests that larger binding propensities within the nucleolus may explain the larger fluorescence and the observed recovery curves. However, more experimentation is needed to exclude that the effect is a consequence of smaller diffusion coefficients or smaller release propensities within the nucleolus. In particular, observation of recovery curves for a mutant with reduced binding affinity would help establish that the observed behavior is not due to slower diffusion (if larger fluorescence intensity in nucleoli was due to slower diffusion, the same effect should be observed for mutants with reduced binding affinity).

VI. CONCLUSIONS

This paper discussed stochastic modelling and simulation of protein diffusion and binding within cell nuclei, and their applications to the study of FRAP experiments. A continuous stochastic model was proposed along with a suitable discrete approximation that is well suited for numerical implementation. Based on the discrete approximation, which is supported by theoretical convergence guarantees, we plan to extend the model as to include interactions among particles and specific recruitment mechanisms onto DNA. The current implementation of the method allowed us to carry out a qualitative analysis of FRAP experimental data from mammalian cancerous cells. In the future, computational speed-up will be pursued so as to turn our simulator into a tool for systematic quantitative data analysis. In addition, theoretical analysis of our simulation method will be performed in the attempt of establishing statistical approximation error bounds.

ACKNOWLEDGEMENTS

The authors would like to thank Andreas Miliadis-Argeitis for useful discussions about FRAP analysis, and Georgia Xouri for providing experimental data and assistance.

REFERENCES

- [1] D. Axelrod, D.E. Koppel, J. Schlessinger, E. Elson and W.W. Webb, "Mobility measurement by analysis of fluorescence photobleaching recovery kinetics". *Biophys. J.* No.16, pp.1055-1069, 1976.
- [2] G.T. Balls and S.B. Baden, "A large scale Monte Carlo simulator for cellular microphysiology", *Proceedings of the 18th International Parallel and Distributed Processing Symposium (IPDPS)*, 2004.
- [3] J. Beaudouin, F. Mora-Bermdez, T. Klee, N. Daigle and J. Ellenberg, "Dissecting the contribution of diffusion and interactions to the mobility of nuclear proteins". *Biophys J.*, 15;90(6), pp.1878-94. Mar. 2006. Epub 30 Dec. 2005.
- [4] S.P. Bell and A.Dutta, "DNA replication in eukaryotic cells". *Annu. Rev. Biochem.*, 71, pp.333-374, 2002.

- [5] J.J. Blow and A. Dutta, "Preventing re-replication of chromosomal DNA". *Nat. Rev. Mol. Cell. Biol.*, 6, pp.476-486, 2005.
- [6] G. Carrero, D. McDonald, E. Crawford, G. de Vries and M.J. Hendzel, "Using FRAP and mathematical modeling to determine the in vivo kinetics of nuclear proteins". *Methods*, No.29, pp.14-28, 2003.
- [7] J. Essers, A.B. Houtsmuller and R. Kanaar, "Analysis of DNA recombination and repair proteins in living cells by photobleaching microscopy". *Methods Enzymol.*, 408, pp.463-485, 2006.
- [8] A.B.Houtsmuller, "Fluorescence Recovery after Photobleaching: Application to Nuclear Proteins". *Adv.Biochem.Engin./Biotechnol.*, No.95, pp.177-199, 2005.
- [9] A.B. Houtsmuller and W. Vermeulen, "Macromolecular dynamics in living cell nuclei revealed by fluorescence redistribution after photobleaching". *Histochem. Cell. Biol.*, No.115, pp.13-21, 2001.
- [10] H.J. Kushner and P.G. Dupuis, *Numerical methods for stochastic control problems in continuous time*. Springer, New York (USA), 1992.
- [11] J. Lippincott-Schwartz, J.F. Presley, K.J.M. Zaal, K. Hirschberg, C.D. Miller and J. Ellenberg, "Monitoring the dynamics and mobility of membrane proteins tagged with Green Fluorescent Protein". In *Green Fluorescent Proteins*, Methods in Cell Biology series, K.F. Sullivan and S.A. Kay eds., Vol.58, pp.261-281, Academic Press, 1999.
- [12] J. Lippincott-Schwartz, E. Snapp and A. Kenworthy, "Studying protein dynamics in living cells". *Nat. Rev. Mol. Cell. Biol.*, 2, pp.444-456, 2001.
- [13] Y.J. Machida, J.L. Hamlin and A. Dutta, "Right place, right time, and only once: replication initiation in metazoans". *Cell*, 123, pp.13-24, 2005.
- [14] H. Nishitani, S. Taraviras, Z. Lygerou and T. Nishimoto, "The human licensing factor for DNA replication Cdt1 accumulates in G1 and is destabilized after initiation of S-phase". *J. Biol. Chem.*, 276, 44905-44911, 2001.
- [15] R.D. Phair, S.A. Gorski and T. Misteli, "Measurement of dynamic protein binding to chromatin in vivo, using photobleaching microscopy". *Methods Enzymol.*, 375, pp.393-414, 2004.
- [16] R.D. Phair and T. Misteli, "Kinetic modelling approaches to in vivo imaging". *Nat Rev Mol Cell Biol*, 2(12), pp.898-907 Dec. 2001, Review.
- [17] R.D. Phair, P. Scaffidi, C. Elbi, J. Vecerová, A. Dey, K. Ozato, D.T. Brown, G. Hager, M. Bustin and T. Misteli, "Global nature of dynamic protein-chromatin interactions in vivo: three-dimensional genome scanning and dynamic interaction networks of chromatin proteins". *Mol Cell Biol.*, 24(14), pp.6393-402, July 2004.
- [18] A. Politi, M.J. Moné, A.B. Houtsmuller, D. Hoogstraten, W. Vermeulen, R. Heinrich and R. van Driel, "Mathematical modeling of nucleotide excision repair reveals efficiency of sequential assembly strategies". *Molecular Cell*, Vol.19, 679-690, September 2005.
- [19] M. Prandini and J. Hu, "Stochastic reachability: Theory and numerical approximation". In C.G. Cassandras, J. Lygeros eds., *Stochastic Hybrid Systems*, CRC press, Control Engineering Series, pp.107-138, 2007.
- [20] G. Rabut and J. Ellenberg, "Photobleaching techniques to study mobility and molecular dynamics of proteins in live cells: FRAP, iFRAP and FLIP". In R.D. Goldman and D.L. Spector (Eds.), *Live Cell Imaging: A Laboratory Manual Vol. 1*, Cold Spring Harbor Laboratory Press, Cold Spring Harbor, pp.101-127, 2005.
- [21] B.M. Slepchenko, J.C. Schaff, I. Macara and L.M. Loew, "Quantitative cell biology with the Virtual Cell", *TRENDS in Cell Biology*, Vol.13, No.11, pp.570-576, November 2003.
- [22] B.L. Sprague and J.G. McNally, "FRAP analysis of binding: proper and fitting". *Trends Cell. Biol.*, 15, pp.84-91, 2005.
- [23] J.S. van Zon and P.R. ten Wolde, "Green's-function reaction dynamics: A particle based approach for simulating biochemical networks in time and space". *Journal of Chemical Physics*, Vol.123, 2005.
- [24] J.S. van Zon and P.R. ten Wolde, "Simulating biochemical networks at the particle level and in time and space: Green's function reaction dynamics". *Physical review letters*, Vol.94, 2005.
- [25] G. Xouri, A. Squire, M. Dimaki, B. Geverts, P.J. Vermeer, S. Taraviras, H. Nishitani, A.B. Houtsmuller, P.I.H. Bastiaens and Z. Lygerou, "Cdt1 associates dynamically with chromatin throughout G1 and recruits Geminin onto chromatin". *The EMBO Journal*, 26, pp.1303-1314, 2007.